Shipley, T.H., Ogawa, Y., Blum, P., and Bahr, J.M. (Eds.), 1997
Proceedings of the Ocean Drilling Program, Scientific Results, Vol. 156

13. GEOCHEMISTRY OF SEDIMENTS AND AUTHIGENIC MINERALS IN AND AROUND THE DÉCOLLEMENT ZONE OF THE NORTHERN BARBADOS RIDGE ACCRETIONARY PRISM[1]

T. Ito,[2] K. Yamaguchi,[3] K. Komuro,[3] Y. Ogawa[3]

ABSTRACT

Chemical analyses for major and trace constituents of authigenic minerals and sediments collected in the northern Barbados Ridge during Ocean Drilling Program Leg 156 have been carried out. In addition to Mn enrichments previously reported, Cu enrichments were identified in this study.

Two kinds of Mn enrichments of rhodochrosite and amorphous Mn oxide occur at Site 948. Both of them have rare-earth element (REE) abundances similar to the North American Shale Composites and typical sediments recovered during Leg 156. Cu enrichments occur just above the décollement zone at Site 948, and also just above an inferred thrust based on the drastic change in interstitial-water chemistry at Site 949. The Cu-enriched parts are characterized by K, Ba, Cr, and light REE depletions.

INTRODUCTION

The northern Barbados Ridge accretionary complex (Figs. 1, 2) is an ideal area to study the origin and migration processes of water and accompanying elements in accretionary complexes, because drilling has penetrated the décollement zone (Legs 78A, 110, and 156). In recent years, much attention has been paid to geochemical studies of fluids and authigenic minerals in accretionary complexes to achieve this scientific goal (e.g., Gieskes et al., 1990; Vrolijk and Sheppard, 1991; Kastner et al., 1991). Although trace-element compositions of authigenic minerals and sediments are also important in the understanding of geochemistry during accretionary processes, only the major-element chemistry of bulk sediments was presented for the Barbados accretionary complex by Wang et al. (1990). Here we report the trace-element chemical compositions, including rare-earth element (REE) abundances, in addition to major constituents for authigenic minerals and bulk sediments.

METHODS

Sediment samples composed of several color fractions were separated macroscopically, without washing. Each sample was powdered using an agate mortar after drying at 60°C overnight, and was completely dissolved by adding HNO_3 (0.5 ml), $HClO_4$ (0.2 ml) and HF (1 ml) for all samples except amorphous Mn-enriched samples, and HCl (1ml), HNO_3 (0.5 ml), $HClO_4$ (0.2 ml), and HF (0.2 ml) for amorphous Mn-enriched samples to closed teflon vials for 10 hr at 110°C, after weighing samples accurately (nearly 80 mg). The sample solutions were dried in an open system and were made up in a final solution of 5% HNO_3. All element compositions except REEs were analyzed using inductively coupled plasma-atomic emission spectroscopy (ICP-AES, Jarrell Ash ICAP-757V). REEs were analyzed using inductively coupled plasma-mass spectrometry (ICP-MS, Yokogawa Hewlett Packard PMS2000) at the Chemical Analysis Center, the University of Tsukuba. Calibrations were performed using solution standards and standard rock samples from the Geological Survey of Japan (JGb1, JG1a, JG2, JB1a, JB2, and JSd3) for REEs and the other elements analyses.

Data on the chemical composition of sediments of Sites 948 and 949 are given in Tables 1 and 2. REE contents are presented in Table 3.

CHEMICAL COMPOSITION

Lithostratigraphic summaries with authigenic mineral occurrences for Sites 948 and 949 are presented in Figures 3 and 4.

Site 948

The chemical compositions of authigenic minerals and bulk sediments of Sites 948 are presented in Figure 5.

The major constituent Al, Fe, Mg, and Na have nearly constant values throughout the core. Ca content varies depending on the contribution of fossiliferous carbonates. K content decreases near the upper boundary of the décollement zone, but decreases at 566.9 m below seafloor (mbsf) because of dilution by high carbonate contents.

Contents of four elements (Mn, Cu, Cr, and Ba) fluctuate greatly at Site 948.

Mn enrichments (~3.5–13 wt%) at Site 948 are characterized by two types. One is white in color and is composed of rhodochrosite, identified using X-ray powder diffraction. This first type of Mn enrichment occurs at 423.2 and 472.7 mbsf, which corresponds to a horizon above the décollement zone. The second type of Mn enrichment is black (Fig. 6). This type of manganese enrichment is amorphous, using X-ray powder diffraction, and occurs at 500 and 509.3 mbsf within the décollement zone. The second types have high Ba contents (1400–2200 ppm). Both types of Mn-enriched rhodochrosite and amorphous Mn oxides also have REE patterns similar to the North American Shale Composites (NASC) and typical sediments from Leg 156, regardless of mineralogy (Fig. 7).

Cu enrichment (~1.3 wt%) was first identified in the accretionary complexes. At Site 948, Cu enrichment occurs at 494.9 mbsf, which corresponds to just above the décollement zone. Chemically, the depletion of K, Ba, and Cr are characteristic of the Cu-enriched sediments. In addition, these sections are also depleted in REEs, especially in light REEs (Fig. 8).

[1]Shipley, T.H., Ogawa, Y., Blum, P., and Bahr, J.M. (Eds.), 1997. *Proc. ODP, Sci. Results*,156: College Station, TX (Ocean Drilling Program).

[2]Faculty of Education, Ibaraki University, Mito, Ibaraki, 310, Japan. tito@mito.ipc.ibaraki.ac.jp

[3]Institute of Geoscience, University of Tsukuba, Tsukuba, Ibaraki, 305, Japan.

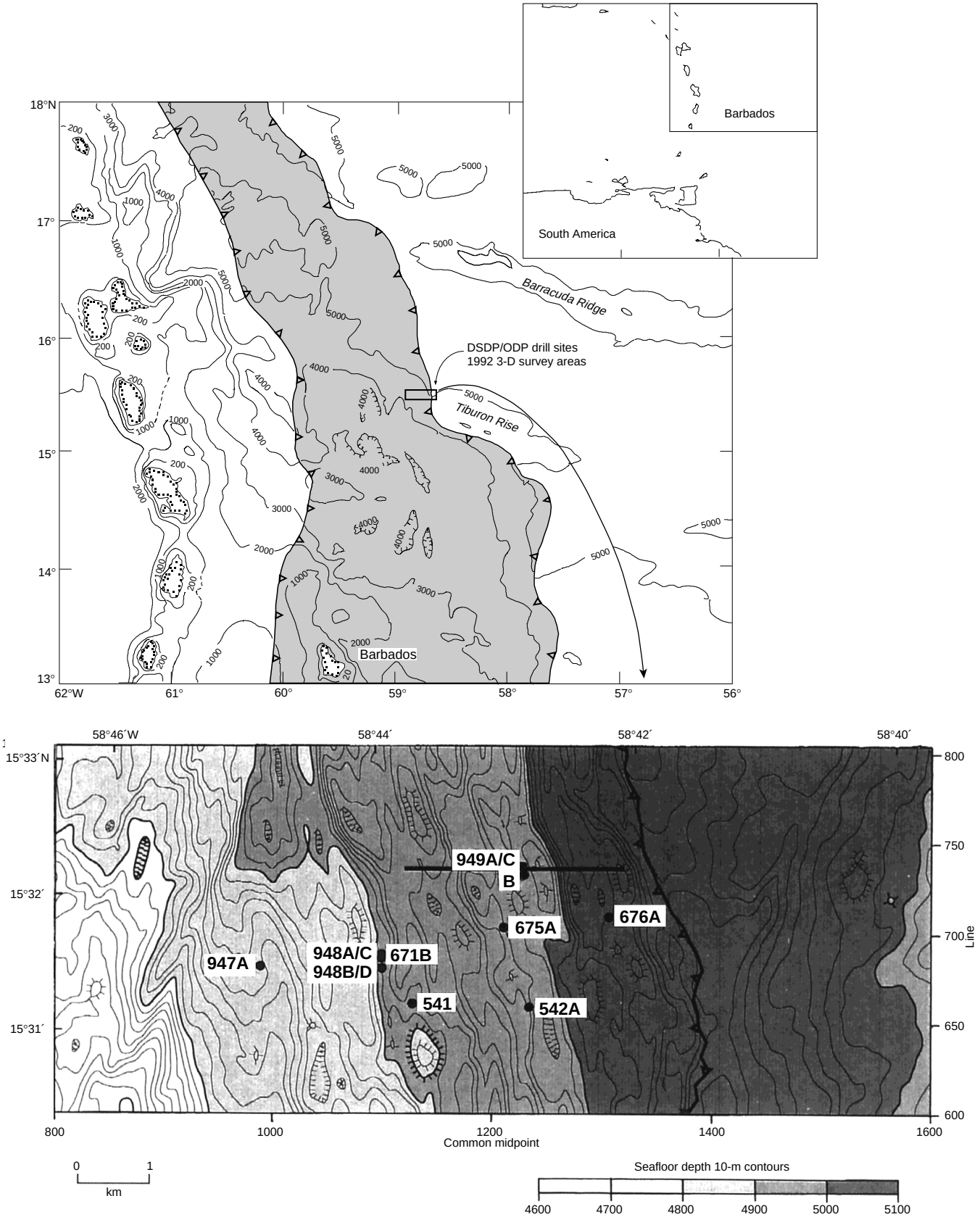

Figure 1. Location map showing the area around Sites 948 and 949. The frontal thrust (barbed line) and Deep Sea Drilling Project (DSDP) and other drill sites are shown. Modified from Shipboard Scientific Party (1995a, 1995c).

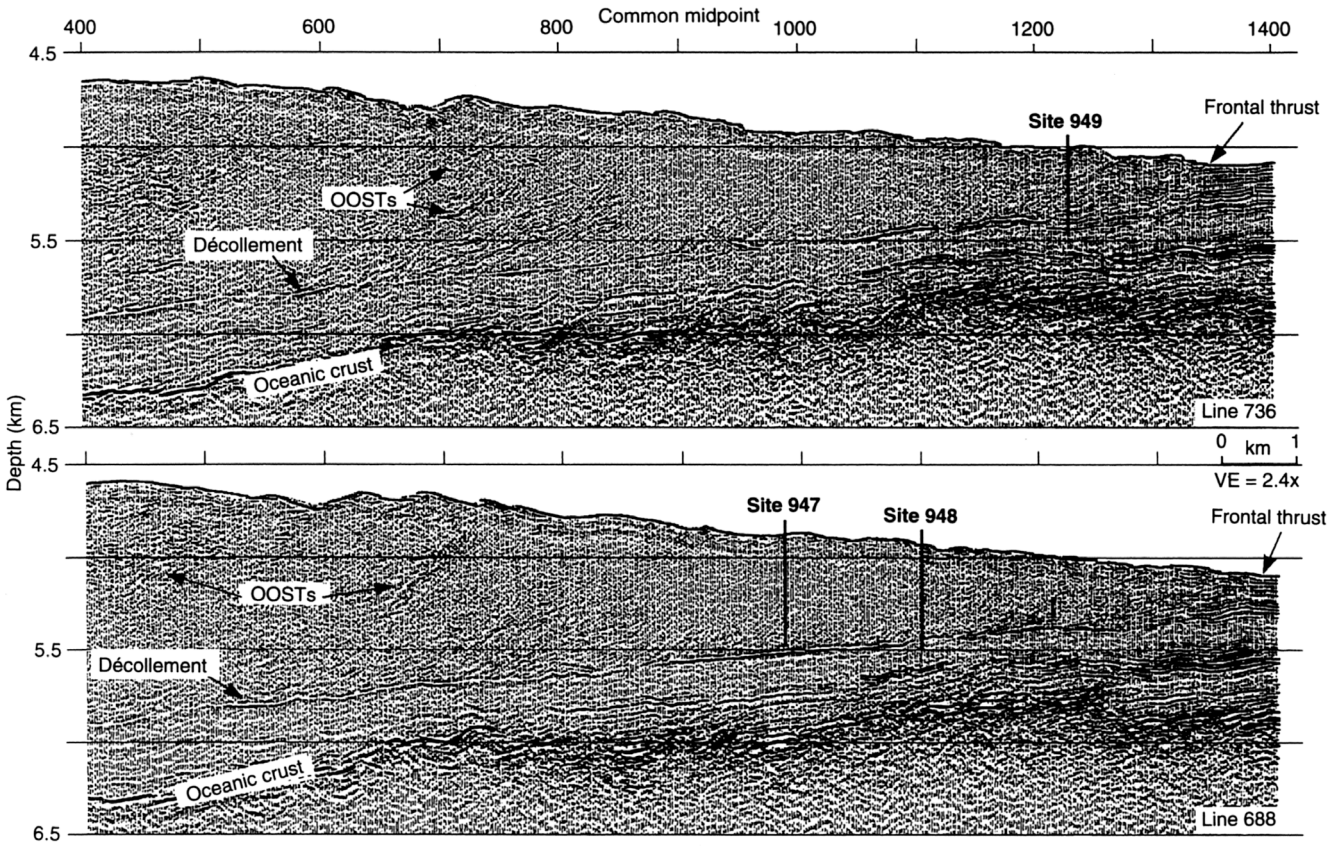

Figure 2. Depth section of three-dimensional seismic images around Sites 948 and 949. This figure is adopted from Moore et al. (1995).

The vertical profile of Cr content is similar to the K-content pattern at Site 948. From similar values at 590 to 500 mbsf, Cr content decreases abruptly from 90 to 10 ppm at the upper boundary of the décollement zone, and increases monotonically toward the upper layer. Several Cr-depleted parts are also poor in REEs, especially in light REEs, regardless of Cu content (Fig. 8).

Site 949

The chemical composition of bulk sediments and authigenic mineral of Sites 949 is presented in Figure 9.

It is hard to understand totally the trend of chemical composition at Site 949 because of poor core recovery. The ranges of fluctuation are similar to those at Site 948 for most of the elements.

Although no abnormal Mn enrichment occurs at this site, Cu enrichment (~3.3 wt%) was present at 284.4 mbsf (Fig. 10), which corresponds to just above the inferred thrust, where the chemical composition of interstitial water changed drastically (Shipboard Scientific Party, 1995c). Similar to the case at Site 948, the Cu-enriched part was characteristically depleted in K, Ba, Cr, and light REEs.

SUMMARY

Studies of bulk chemical composition have revealed geochemical features of sediments recovered from Leg 156 sites. Several important characteristics have been identified.

1. Both types of Mn enrichments, rhodochrosite and amorphous Mn oxide, are identical to the NASC and typical sediments from Leg 156 in terms of REE abundance. Only black amorphous Mn oxide is accompanied by a Ba enrichment.
2. Cu-enriched parts (~1.3–3.3 wt%) were identified from around the décollement zone or thrust, indicated by drastic changes in interstitial-water chemistry. They are characterized chemically by K, Ba, Cr, and light REE depletions.

ACKNOWLEDGMENTS

The authors would like to thank Ms. Y. Takeuchi of the Chemical Analysis Center, the University of Tsukuba, for supporting the chemical analyses.

REFERENCES

Gieskes, J.M., Vrolijk, P., and Blanc, G., 1990. Hydrogeochemistry of the northern Barbados accretionary complex transect: Ocean Drilling Program Leg 110. *J. Geophys. Res.*, 95:8809–8818.

Gromet, L.P., Dymek, R.F., Haskin, L.A., and Korotev, R.L., 1984. The "North American Shale Composite": its compilation, major and trace elements characteristics. *Geochim. Cosmochim. Acta,* 48:2469–2482.

Haskin, L.A., Haskin, M.A., Frey, F.A., and Wildman, T.R., 1968. Relative and absolute terrestrial abundances of the rare earths. *In* Ahrens, L.H. (Ed.), *Origin and Distribution of the Elements:* New York (Pergamon), 889–912.

Kastner, M, Elderfield, H. Martin, J. B., 1991. Fluids in convergent margins: what do we know about their composition, origin, role in diagenesis and importance for oceanic chemical fluxes? *Phil. Trans. R. Soc. Lond.* A, 335: 243–259.

Moore, G.F., Zhao, Z., Shipley, T.H., Bangs, N., and Moore, J.C., 1995. Structural setting of the Leg 156 area, northern Barbados Ridge accre-

tionary prism. *In* Shipley, T.H., Ogawa, Y., Blum, P., et al., *Proc. ODP, Init. Repts.*, 156: College Station, TX (Ocean Drilling Program), 13–27.
Shipboard Scientific Party, 1995a. Introduction. *In* Shipley, T.H., Ogawa, Y., Blum, P., et al., *Proc. ODP, Init. Repts.*, 156: College Station, TX (Ocean Drilling Program), 3–11.
————, 1995b. Site 948. *In* Shipley, T.H., Ogawa, Y., Blum, P., et al., *Proc. ODP, Init. Repts.*, 156: College Station, TX (Ocean Drilling Program), 87–192.
————, 1995c. Site 949. *In* Shipley, T.H., Ogawa, Y., Blum, P., et al., *Proc. ODP, Init. Repts.*, 156: College Station, TX (Ocean Drilling Program), 193–257.
Vrolijk, P., and Sheppard, S.M.E., 1991. Syntectonic carbonate veins from the Barbados accretionary prism (ODP Leg 110): record of palaeohydrology. *Sedimentology*, 38:671–690.
Wang, Y.C., Gieskes, J.M., and Musoke, L., 1990. Bulk chemical analysis of sediments—Hole 671B. *In* Moore, J.C., Mascle, A. et al., *Proc. ODP, Sci. Results*, 110: College Station, TX (Ocean Drilling Program), 179–188.

Date of initial receipt: 5 February 1996
Date of acceptance: 16 July 1996
Ms 156SR-022

Table 1. Chemical composition of bulk sediments and authigenic minerals, Site 948.

Core, section, interval (cm)	Depth (mbsf)	Working no.	Al (%)	Ba (ppm)	Ca (%)	Cr (ppm)	Cu (ppm)	Fe (%)	K (%)	Li (ppm)	Mg (%)	Mn (%)	Na (%)	P (ppm)	Sr (ppm)	Ti (ppm)	V (ppm)	Zn (ppm)
156-948B-																		
1H-3, 54–56	3.5	1	6.76	278	1.31	87	80	3.79	1.53	53	1.27	0.123	1.66	504	596	3,202	125	90
156-948C-																		
1H-2, 89–91	2.4	2	9.84	482	1.00	125	101	5.44	1.93	72	1.72	0.369	1.67	600	154	4,788	172	132
1H-6, 99–101	8.5	3	10.12	393	1.76	121	71	5.82	2.03	78	1.69	0.108	1.76	590	182	4,780	177	138
2X-2, 85–87	423.2	4	8.74	253	1.25	123	27	5.30	1.85	59	1.71	6.000	0.91	720	102	3,733	135	120
3X-3, 13–15	436.6	5	10.31	278	0.80	88	62	5.56	1.97	73	1.84	0.157	1.39	584	118	5,181	183	138
4X-3, 102–106	444.1	6	9.29	225	4.83	81	67	4.70	1.65	74	1.81	0.137	1.24	396	257	4,237	180	114
4X-4, 63–66	445.2	7	7.63	245	11.26	89	36	4.26	1.62	63	1.27	0.534	0.78	519	525	3,065	111	95
5X-4, 137–139	455.7	8	9.64	213	1.57	77	53	5.04	1.64	84	1.79	0.155	1.26	350	149	4,650	129	100
6X-2, 61–63	461.5	10	10.69	241	0.54	83	80	5.94	1.79	106	1.69	0.156	1.10	446	103	4,478	120	119
6X-3, 127–129	463.7	11	9.52	179	0.86	53	38	5.29	1.38	96	2.11	0.293	1.49	427	100	4,413	140	109
7X-3, 71–73	472.7	12	6.69	193	2.53	76	203	3.25	1.14	67	1.89	13.150	0.94	469	85	3,222	109	92
7X-3, 123–126	473.2	13	9.77	229	0.72	59	48	5.63	1.45	88	2.00	0.156	1.42	435	106	4,947	133	104
8X-5, 122–124	485.9	14	9.24	288	1.33	49	76	6.39	1.18	84	2.05	0.120	1.67	433	127	5,168	108	117
9X-4, 6–9	493.0	15	9.56	37	2.29	10	151	4.56	0.52	35	1.90	0.116	2.01	791	407	5,272	55	76
9X-4, 27–30	493.2	16	8.68	289	1.23	47	52	5.82	1.06	74	2.17	0.353	1.63	479	120	4,996	147	110
9X-5, 53–55	494.9	17	8.07	43	2.21	12	13,000	6.45	1.23	41	1.61	0.098	2.04	141	141	6,926	385	177
10X-1, 74–77	498.8	18	8.65	57	2.77	42	61	6.77	0.66	36	1.44	0.078	2.20	233	201	6,352	301	115
10X-2, 44–46	500.0	19ocher	9.34	217	1.18	71	99	4.87	1.30	81	1.68	0.193	1.64	629	152	3,907	111	123
	500.0	19black	8.31	1,454	1.16	80	127	4.70	1.19	73	1.62	4.763	1.62	570	183	3,726	303	121
10X-2, 57–59	500.2	20	9.23	259	1.10	79	92	5.26	1.24	75	1.59	0.374	1.44	553	144	4,295	136	126
10X-3, 31–33	501.4	21	9.39	272	0.99	90	95	4.95	1.23	78	1.57	0.337	1.41	490	127	4,040	137	128
10X-3, 110–150	502.4	22	8.85	467	0.82	88	91	4.70	1.16	78	1.59	0.729	1.29	415	125	3,735	150	124
11X-2, 13–15	509.3	24ocher	9.65	423	0.50	100	238	4.90	1.33	67	1.13	0.149	1.07	408	116	3,814	131	122
	509.3	24black	9.03	2,128	0.53	89	430	4.75	1.25	63	1.17	3.677	1.06	467	170	3,748	241	128
11X-5, 25–27	514.0	25	8.48	288	0.32	76	37	5.01	1.42	42	0.96	0.038	1.18	209	108	4,008	150	96
12X-5, 76–80	524.2	26	8.80	429	0.48	97	42	3.95	1.76	75	0.94	0.078	1.09	346	115	4,343	167	187
12X-6, 3–5	524.9	27greenish	10.03	333	0.34	98	46	5.03	2.18	72	1.26	0.025	0.95	224	107	3,809	163	106
	524.9	27gray	10.55	320	0.30	137	47	4.02	2.32	81	1.05	0.023	1.01	177	117	3,425	163	136
13X-CC, 7–9	536.4	28greenish	11.03	399	0.31	101	39	5.01	2.21	100	1.09	0.018	0.86	321	109	4,177	188	133
	536.4	28gray	11.75	324	0.29	105	34	4.12	2.45	104	0.98	0.020	0.90	202	132	4,300	210	154
14X-2, 17–19	537.8	29	8.86	312	0.32	394	29	13.16	2.20	89	0.83	0.021	0.77	245	943	2,541	70	128
14X-5, 48–50	542.6	30	11.11	368	0.32	106	28	5.54	2.26	102	1.24	0.019	0.86	259	109	4,183	190	120
15X-2, 87–89	547.8	31	11.39	546	0.39	121	120	4.99	1.44	132	1.25	0.022	0.88	419	954	933	175	277
15X-7, 25–27	554.7	32	9.57	335	0.36	97	38	6.96	2.36	72	1.23	0.037	0.88	292	114	4,082	162	108
17X-2, 120–150	566.9	33	1.89	1,180	24.60	38	18	2.78	0.31	37	0.65	1.042	0.46	357	1,186	3,506	50	33
17X-4, 81–84	569.4	34	10.41	370	2.61	118	129	4.55	1.74	120	1.12	0.029	0.90	536	218	4,355	168	137
18X-2, 68–70	575.5	35	9.68	385	0.37	99	46	3.88	2.11	86	0.99	0.019	0.91	288	120	5,197	192	177
19X-6, 72–75	591.0	36	8.18	535	10.24	111	57	4.36	1.40	81	0.96	0.131	0.75	332	656	3,555	133	105
19X-7, 33–36	592.1	37	10.34	338	0.93	100	40	5.39	2.26	86	1.13	0.092	0.79	288	161	4,943	175	390

Table 2. Chemical composition of bulk sediments and authigenic minerals, Site 949.

Core, section, interval (cm)	Depth (mbsf)	Working no.	Al (%)	Ba (ppm)	Ca (%)	Cr (ppm)	Cu (ppm)	Fe (%)	K (%)	Li (ppm)	Mg (%)	Mn (%)	Na (%)	P (ppm)	Sr (ppm)	Ti (ppm)	V (ppm)	Zn (ppm)
156-949A-																		
1H-2, 61–64	2.1	38	8.21	407	3.75	99	98	4.91	2.14	67	1.63	0.320	2.11	454	236	3,962	151	104
156-949B-																		
1X-2, 9–11	245.7	39	9.37	225	0.95	87	45	5.40	1.71	79	1.80	0.160	1.35	369	117	4,281	139	325
2X-6, 58–60	261.9	40	10.27	246	0.52	10	74	66.07	1.79	95	1.59	0.349	1.18	572	101	4,240	148	133
3X-3, 135–137	267.9	41	10.21	243	0.64	105	55	5.61	1.81	93	1.74	0.189	1.23	785	105	4,223	143	117
4X-CC, 19–21	275.0	42	9.47	157	0.84	44	345	3.45	1.46	90	2.31	0.180	1.89	260	142	5,215	100	122
5X-2, 8–10	284.4	43greenish	7.97	12	1.40	11	33,400	2.31	0.53	64	2.28	0.128	1.73	431	119	3,718	129	189
	284.4	43matrics	8.26	192	0.84	25	97	3.90	0.86	77	2.41	0.131	1.81	240	110	4,530	194	102
5X-5, 3–5	288.8	44	8.81	426	0.83	78	69	4.85	1.68	80	1.88	0.210	1.71	419	149	4,124	147	121
5X-7, 40–42	292.2	45	8.44	311	0.99	55	88	5.32	1.13	66	2.05	0.191	1.67	502	125	4,190	118	122
7X-2, 60–62	304.2	46	9.65	668	2.84	7	43	1.66	0.86	49	1.95	0.103	2.21	198	240	2,697	108	93
13X-2, 36–39	352.1	47	9.68	196	1.15	76	51	5.11	1.69	87	1.82	0.195	1.46	449	126	4,400	138	113
13X-2, 92–96	352.6	48	10.88	232	0.50	110	58	5.49	2.48	110	1.57	0.085	1.33	471	147	4,591	150	137
14X-3, 72–77	358.6	49	9.44	337	0.70	34	241	4.87	1.36	84	1.89	0.233	1.89	182	109	2,848	82	93
14X-6, 67–69	363.1	50	10.35	221	0.48	82	31	5.89	1.83	91	1.60	0.081	1.23	469	108	4,499	123	108
15X-2, 48–50	361.9	51	9.73	183	0.58	72	49	5.15	1.58	95	1.96	0.159	1.48	391	106	4,242	142	119
15X-4, 21–23	364.6	52	9.37	192	0.61	64	84	5.12	1.45	89	2.08	0.197	1.43	390	108	4,155	116	113
19X-3, 20–22	401.5	53	9.31	216	0.60	92	120	4.83	1.13	84	1.44	0.199	1.33	371	125	3,898	118	138
19X-3, 51–53	401.8	54ocher	9.45	287	0.56	88	90	4.82	1.27	79	1.43	0.199	1.23	413	132	4,287	113	121
	401.8	54brown.	9.52	560	0.55	88	93	4.77	1.26	79	1.46	0.734	1.21	418	142	4,411	140	121
22X-4, 56–58	432.5	55	9.21	402	0.33	92	227	4.25	2.20	69	1.04	0.040	1.19	259	142	4,507	181	2038
22X-6, 59–61	435.5	56	9.92	344	0.38	89	49	5.70	1.80	69	1.35	0.038	1.10	371	124	4,336	139	114
25H-1, 126–128	459.7	57	11.59	382	0.38	116	205	5.25	2.63	124	1.11	0.024	0.96	507	144	4,476	179	191
156-949C-																		
4R-1, 19–21	426.0	58	9.85	426	0.45	99	110	4.85	1.97	81	1.11	0.067	1.27	326	180	4,070	196	169

Table 3. Rare earth element abundance of bulk sediments and authigenic minerals, Sites 948 and 949.,

Core, section, interval (cm)	Depth (mbsf)	Working no.	Sc (ppm)	Y (ppm)	La (ppm)	Ce (ppm)	Pr (ppm)	Nd (ppm)	Sm (ppm)	Eu (ppm)	Gd (ppm)	Tb (ppm)	Dy (ppm)	Ho (ppm)	Er (ppm)	Tm (ppm)	Yb (ppm)	Lu (ppm)
156-948C-																		
2X-2, 85–87	423.2	4	16.3	25.6	35.7	85.4	8.34	33.3	6.41	1.36	5.72	0.81	4.95	0.98	2.71	0.43	2.86	0.43
3X-3, 13–15	436.6	5	23.9	27.2	35.9	81.9	8.96	35.9	7.01	1.73	7.02	1.01	5.85	1.18	3.13	0.45	3.02	0.46
4X-3, 102–106	444.1	6	21.3	21.7	30.5	67.4	7.46	30.2	5.64	1.35	5.84	0.81	4.73	0.90	2.50	0.38	2.51	0.38
6X-3, 127–129	463.7	11	22.5	31.8	26.9	74.8	7.69	28.3	5.92	1.48	5.74	0.93	5.48	1.08	3.01	0.48	3.17	0.53
7X-3, 71–73	472.7	12	17.1	57.3	27.3	73.5	6.72	26.3	5.31	1.43	8.03	1.02	6.72	1.62	5.10	0.93	6.80	1.08
9X-4, 6–9	493.0	15	44.0	4.9	2.6	6.4	0.81	3.6	0.86	0.32	0.94	0.17	1.01	0.21	0.65	0.09	0.75	0.11
9X-4, 27–30	493.2	16	28.3	27.4	24.3	54.6	6.35	25.5	5.49	1.45	5.72	0.91	5.34	1.06	3.05	0.48	3.15	0.47
9X-5, 53–55	494.9	17	34.5	11.2	3.6	9.7	1.04	3.9	1.07	0.42	1.19	0.22	1.68	0.42	1.40	0.27	2.14	0.35
10X-1, 74–77	498.8	18	30.3	9.6	6.3	15.1	1.87	8.0	1.85	0.65	2.14	0.32	1.73	0.41	1.19	0.16	1.21	0.20
10X-2, 44–46	500.0	19ocher	23.1	42.9	41.2	99.1	10.20	41.7	8.32	2.06	8.32	1.26	7.51	1.57	4.64	0.67	4.02	0.64
10X-2, 44–46	500.0	19black	21.6	40.6	38.3	97.9	9.48	40.4	8.35	2.13	7.94	1.18	7.09	1.39	3.79	0.58	3.87	0.66
10X-3, 110–150	502.4	22	22.8	34.3	39.7	100.5	9.61	43.2	8.38	1.94	7.78	1.19	6.96	1.36	3.67	0.57	3.68	0.58
11X-2, 13–15	509.3	24black	19.0	25.0	38.6	105.7	9.33	36.9	6.89	1.75	5.93	0.82	4.77	0.95	2.63	0.39	3.22	0.41
12X-6, 3–5	524.9	27greenish	17.9	19.2	42.8	89.4	9.73	36.4	6.36	1.37	5.38	0.76	4.17	0.76	2.10	0.31	2.37	0.34
12X-6, 3–5	524.9	27gray	17.8	16.6	40.8	88.0	9.54	35.7	5.96	1.25	5.13	0.66	3.82	0.74	2.04	0.31	2.04	0.30
13X-CC, 7–9	536.4	28greenish	19.9	20.9	45.4	103.1	10.85	41.8	7.61	1.62	6.32	0.89	5.16	0.93	2.47	0.39	2.65	0.35
13X-CC, 7–9	536.4	28gray	19.1	14.1	42.2	87.4	9.27	35.3	5.86	1.10	4.55	0.61	3.33	0.62	1.82	0.26	1.96	0.30
15X-2, 87–89	547.8	31	19.9	27.8	56.8	120.6	12.38	47.5	8.18	1.88	7.15	0.98	6.82	1.03	2.65	0.43	2.85	0.39
17X-4, 81–84	569.4	34	19.3	30.3	49.4	110.7	11.91	47.3	8.48	1.97	8.04	1.11	6.62	1.25	3.38	0.45	3.20	0.45
19X-6, 72–75	591.0	36	16.1	27.0	52.7	113.2	11.39	45.2	8.06	1.80	6.73	1.00	5.60	1.03	2.74	0.41	2.69	0.46
156-949B-																		
4X-CC, 19–21	275.0	42	24.8	14.8	15.7	37.8	4.32	17.2	3.48	0.87	3.36	0.53	3.35	0.66	1.81	0.25	1.91	0.28
5X-2, 8–10	284.4	43matrics	33.1	20.1	17.9	44.0	5.13	21.8	4.91	1.29	4.85	0.78	4.59	0.87	2.27	0.36	2.30	0.37
5X-2, 8–10	284.4	43greenish	25.0	15.9	9.3	26.2	3.07	14.6	3.41	0.96	3.87	0.60	3.41	0.64	1.74	0.27	1.96	0.27
5X-5, 3–5	288.8	44	22.0	26.5	28.4	72.8	7.94	32.1	6.10	1.64	6.24	0.97	5.71	1.06	3.03	0.45	2.92	0.48
5X-7, 40–42	292.2	45	24.9	33.1	28.3	68.2	7.78	31.6	6.58	1.74	7.04	1.10	6.53	1.31	3.58	0.57	3.74	0.56

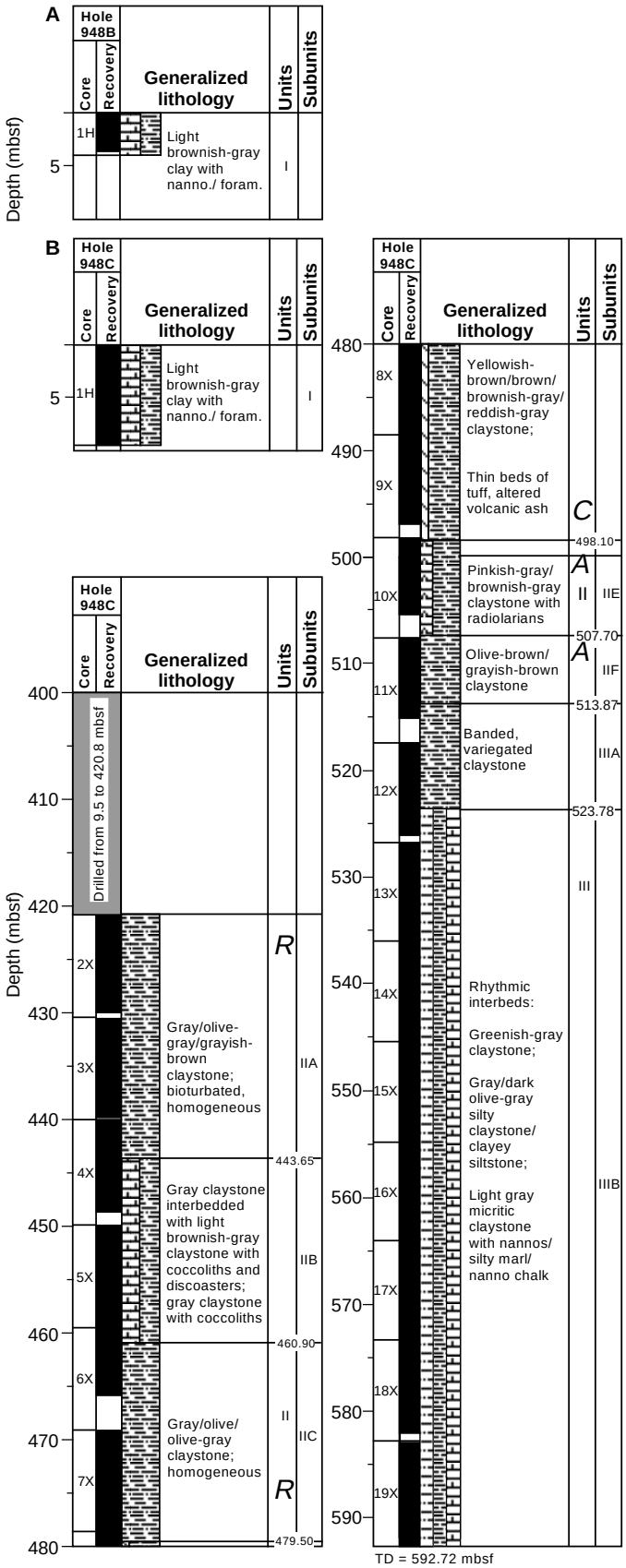

Figure 3. Lithostratigraphic summary for Site 948, adapted from Shipboard Scientific Party (1995b). **A.** Hole 948B. **B.** Hole 948C. In "Units" column, "R," "A," and "C" show occurrences of rhodochrosite, amorphous Mn oxide, and Cu enrichment.

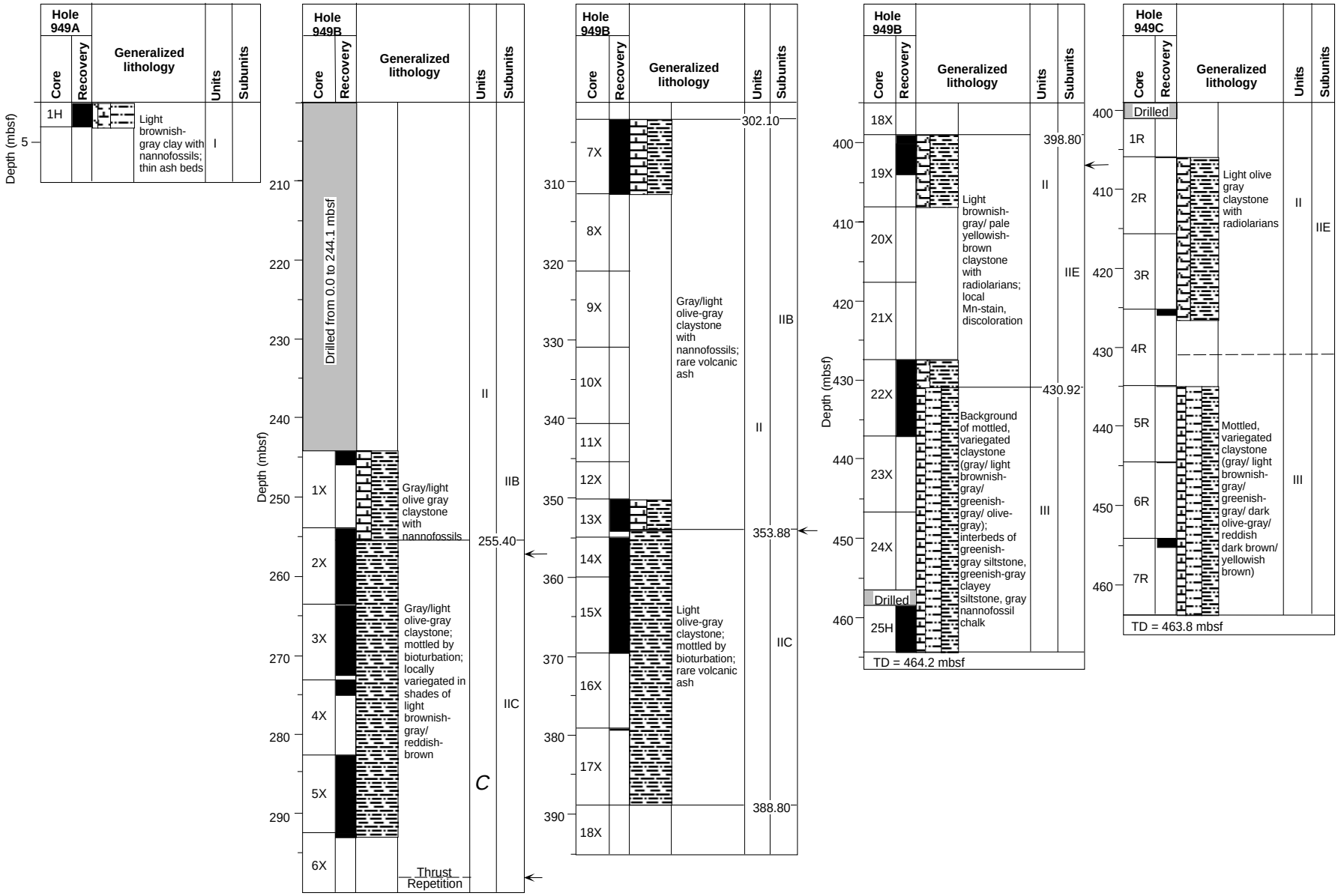

Figure 4. Lithostratigraphic summary for Site 949, adapted from Shipboard Scientific Party (1995c). “C” shows occurrence of Cu enrichment.

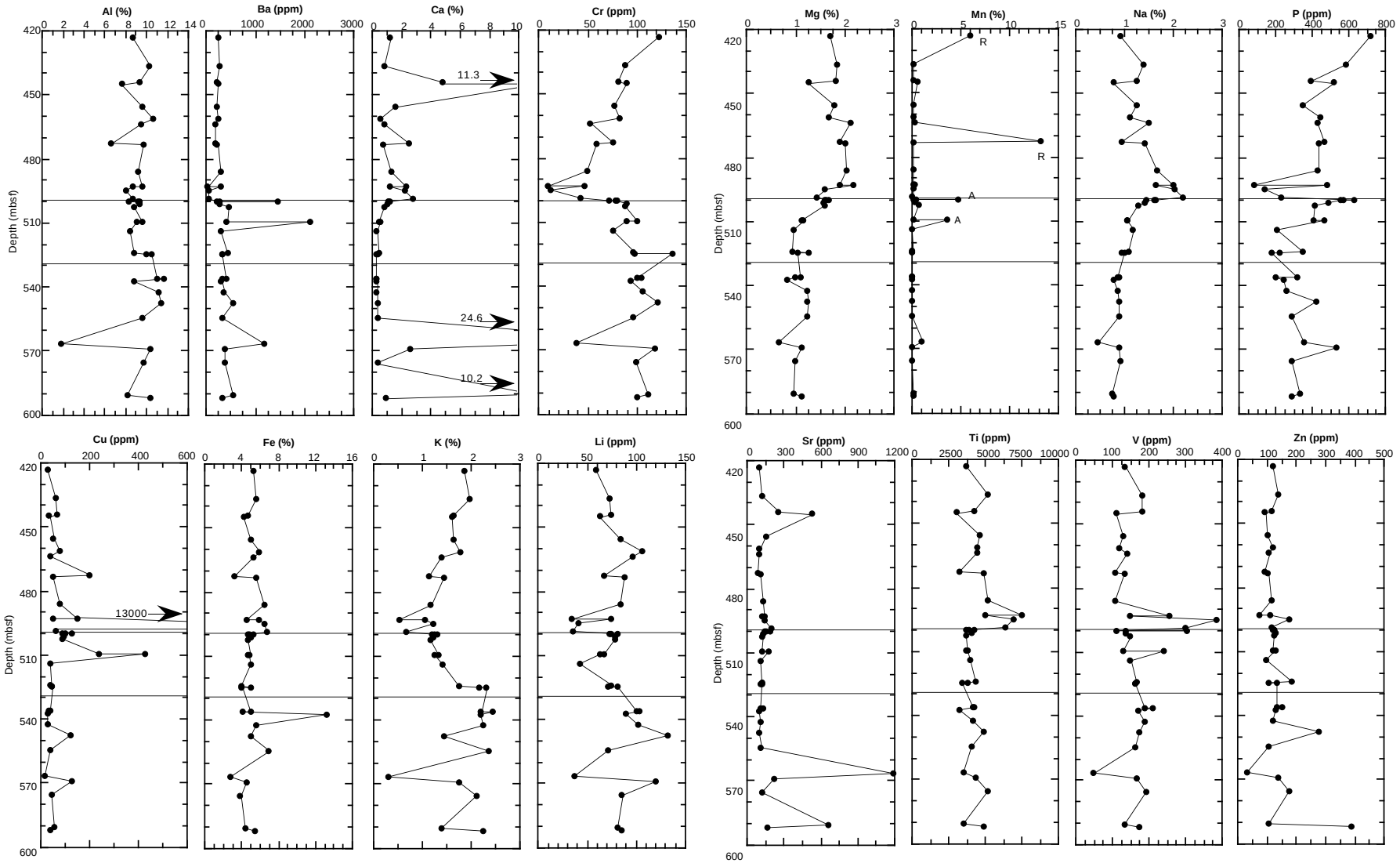

Figure 5. Element composition of bulk sediments and authigenic minerals of Site 948. The area between the two lines corresponds to the décollement zone. In the plot of Mn vs. depth, “R” and “A” indicate rhodochrosite-bearing and amorphous Mn oxide-bearing parts.

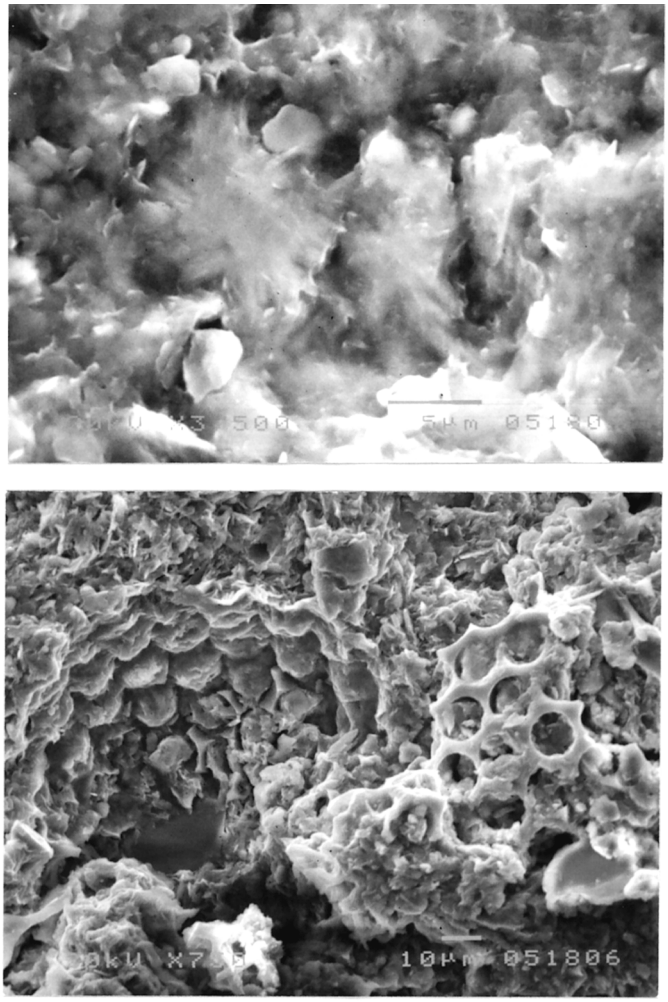

Figure 6. Scanning electron photomicrographs of various morphologies of black amorphous Mn minerals (Sample 156-948C-10X-2, 44−46 cm). Upper part: typical texture of amorphous black Mn oxides. Lower part: Mn oxides forming molds of siliceous fossil tests.

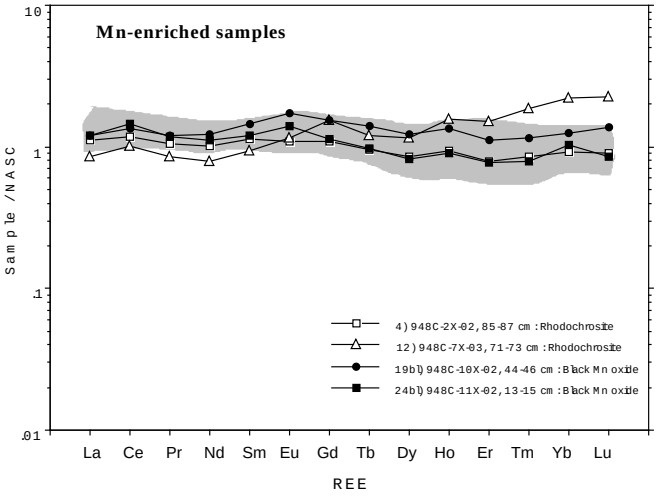

Figure 7. REE abundance of Mn-enriched samples in Leg 156 (open symbols = rhodochrosite-bearing, solid symbols = amorphous Mn oxide-bearing parts). The shaded portion shows the range of REE abundances of typical sediments from Leg 156. REE abundances of North American Shale Composites (NASC) were adapted from Haskin et al. (1968) and Gromet et al. (1984).

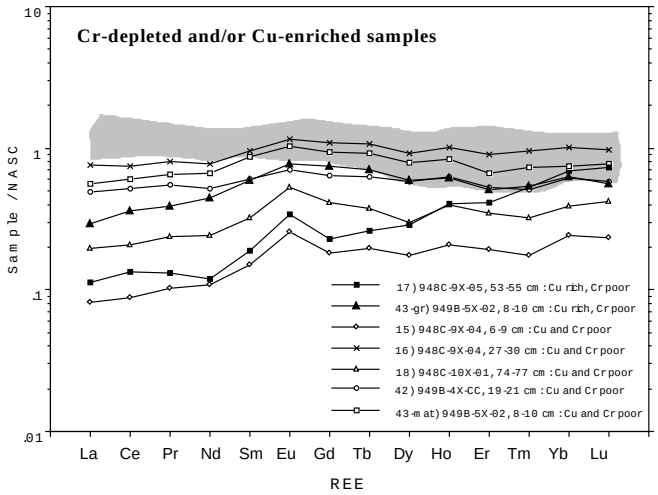

Figure 8. REE abundances of Cr-depleted and/or Cu-enriched samples from Leg 156. All the samples plotted here have low Cr contents, <50 ppm. Solid symbols are Cr-depleted and Cu-enriched samples. Open symbols show Cr and Cu-depleted samples. The shaded portion represents the range of REE abundance of typical sediments from Leg 156.

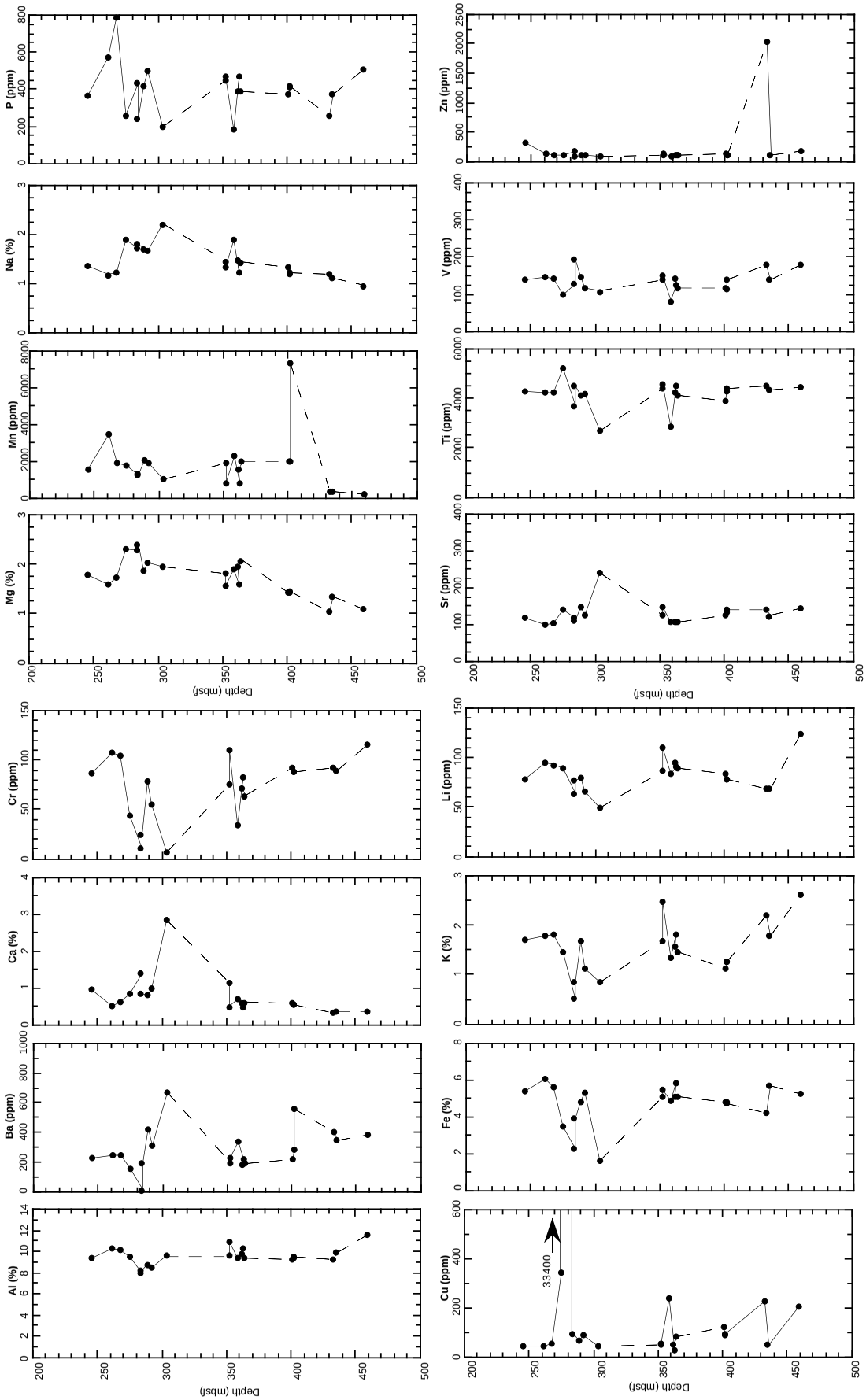

Figure 9. Element compositions of bulk sediments and authigenic minerals from Site 949. Depth shown by dashed line indicates range of no recovery.

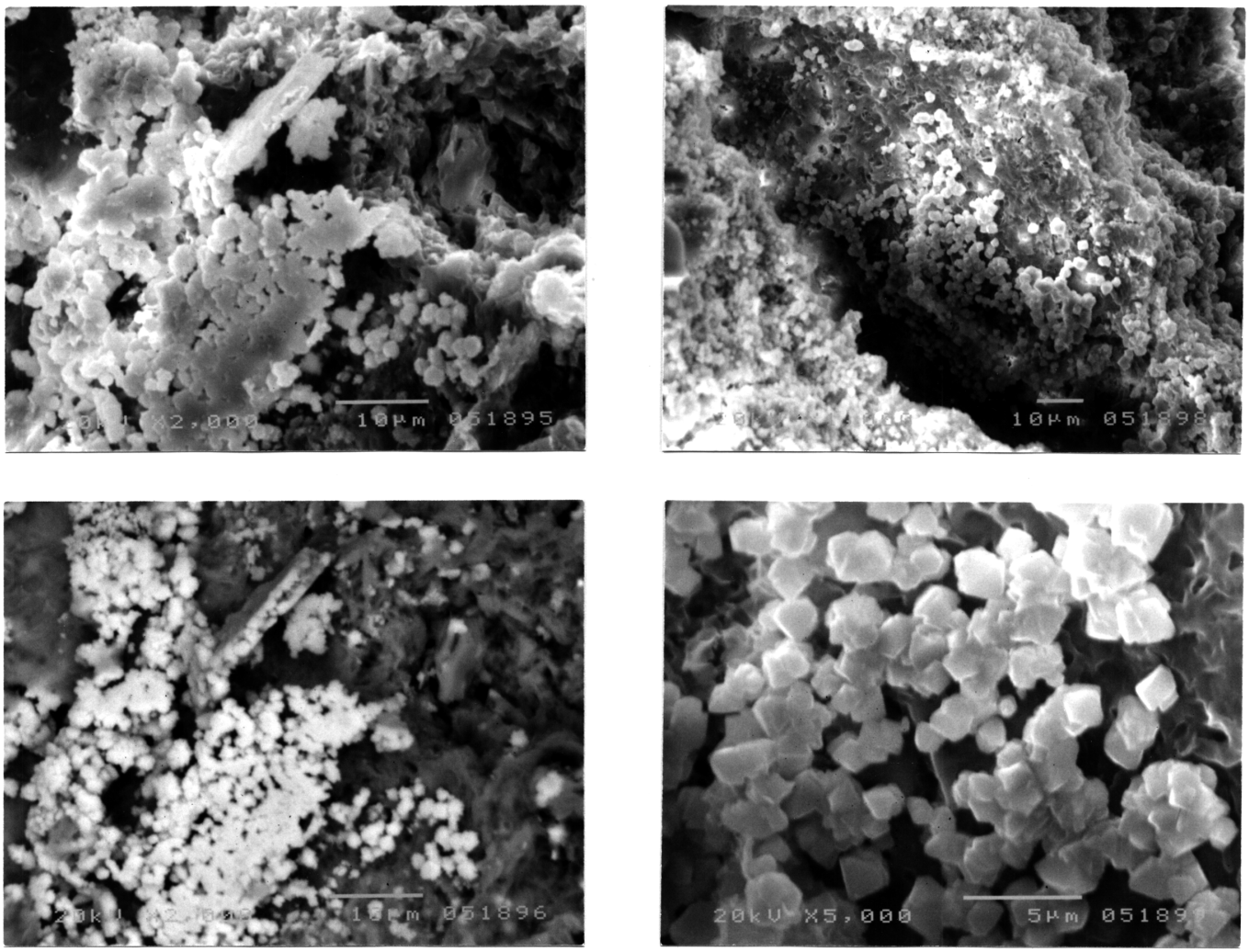

Figure 10. Scanning electron photomicrographs and component image of various morphologies of Cu minerals (Sample 156-949B-5X-2, 8–10 cm). **Upper parts:** aggregate of single grains. **Lower left:** component image of same area as the upper left photomicrograph. White parts correspond to Cu minerals. **Lower right:** close-up of upper right photomicrograph.

Previous Chapter Table of Contents Next Chapter